Light Curve Analysis and Attitude Estimation of Space Objects Focusing on Glint

Yuri Matsushita[(1)], Ryohei Arakawa[(2)], Yasuhiro Yoshimura[(2)], and Toshiya Hanada[(2)]

(1) Kyushu University, 744 Motooka, Nishi-ku, Fukuoka 819-0395(Japan), matsushita.yuri.848@s.kyushu-u.ac.jp
(2) Kyushu University, 744 Motooka, Nishi-ku, Fukuoka 819-0395(Japan)

ABSTRACT

Grasping of dynamic states of space objects such as shape, attitude, and surface properties plays a significant role in removing orbital debris and in monitoring the health of operational satellites. Light Curve Inversion is a cost-effective state estimation technique using light curves, a time history of magnitude obtained by ground-based observations. The problem of this method is, however, that the observer measure only scalar data regardless of plural parameters to be estimated so that estimation accuracy is dependent of the initial values of estimation procedure. This study proposes a high-accurate estimation method using only light curves focusing on their characteristic, especially the sudden change of magnitude, called "glint". Constrained conditions governing glint detection are shown in this paper. They are essential to exclude meaningless values from initial value candidates by setting attitudes in glint detection as the initial state values. Moreover, they realize a high-accurate estimation regardless of the initial values by efficient update of states and covariance matrix with constrains in the estimation filter.

1 Background and Motivation

Active Debris Removal (ADR) is one of the effective measures to maintain and/or reduce the number of orbital debris in Low Earth Orbit (LEO) [1]. Grasping of dynamic states of orbital debris such as their shape, attitude motion, and surface properties plays a significant role in completing ADR missions successfully. It is also beneficial to monitor operational satellites that may collide or break [2].

Light Curve Inversion is a dynamic state estimation technique using light curves, brightness of space objects as a function of time obtained by ground-based observations. Light curves, obtained with inexpensive and widely used devices such as telescopes and CCD cameras, are the more cost-effective information than the conventional ones. This advantage makes it possible to observe a target from multiple points, so that observers can conduct measurement under adverse weather conditions. The main causes of light twinkling observed as light curves are follows:
1. Positional relationship among the Sun, an observer, and a space object,
2. Projected area with respect to the observer direction,
3. Properties of sunlight reflecting surfaces.
These are determined by dynamic states such as shape, attitude, and specular reflectance of the target to define the intensity of light reflected toward the observer. Inversely, observation data as light curves enable to estimate states in a dynamic system. Light Curve Inversion is historically used in the field of astronomy to determine the axis and shape of asteroids [3]. Studies that apply the technology to orbital debris and satellites in operation have been conducted in recent years. The previous study discussed the dynamic state estimation of a space object in GEO from its light curve using Unscented Kalman Filter (UKF) and Multiple-model Adaptive Estimation (MMAE) [4].

In Light Curve Inversion, on the other hand, the observer measure only scalar data of magnitude, regardless of plural parameters to be estimated. Thus, it is known that this estimation method requires the initial attitude and the initial angular velocity of the target that are very near to the true values to realize the high-accurate estimation. To make matters worse, the estimation accuracy decreases significantly considering the limiting magnitude of the telescopes. To avoid those difficulties, the previous studies determined the initial values by using images obtained with radar or adaptive optics [5]. However, imaging by radar is very expensive method due to its larger instruments. Adaptive optics, which is a more reasonable method than radar, have a risk of getting insufficient images for the state estimation because of ambiguity by atmospheric disturbance.

This study proposes a high-accurate estimation method using only light curves without such special instruments by focusing on the characteristic, especially the rapid change of magnitude, called "glint". Glint is a short-term effect in light curves of space objects. It is known that the vicinity of glint has high observability and the large amount of information [6]. The previous study analytically estimated angular velocities from glint time width [7] and rotation axis from the moment of glint detection [8]. However, the problem is that the estimation accuracy rather drops immediately after glint because of its high frequency by using conventional estimation filters. This paper shows constrained conditions of glint detection. It is possible to exclude meaningless values from initial value candidates by understanding the constrains and setting attitudes in glint detection as the initial state values. Moreover, a high-accurate estimation can be performed regardless of the initial values by efficient update of states and covariance matrix with constrains in the estimation filter.

2 Method

This section describes two models of light curves to understand constrains of glint detection. Static Light Curve Model is constructed to find geometric constrains among the Sun, the observer, and the space objects. Quasi-static Light Curve Model is used to make qualitative understanding of dynamics in glint detection.

2.1 Static Light Curve Model

Static Light Curve Model calculates magnitude, apparent area, and γ from attitude described by Euler angles. γ is the angle between the normal vector of the facet ($\boldsymbol{u_n}$) and the bisecting vector ($\boldsymbol{u_h}$) of the sun directional vector ($\boldsymbol{u_{sun}}$) and the observer vector ($\boldsymbol{u_{obs}}$). γ is written as

$$\cos\gamma = \boldsymbol{u_h} \cdot \boldsymbol{u_{n(i)}} \tag{1}$$

where

$$\boldsymbol{u_h} = \frac{\boldsymbol{u_{sun}} + \boldsymbol{u_{obs}}}{\|\boldsymbol{u_{sun}} + \boldsymbol{u_{obs}}\|} \tag{2}$$

Ashikhmin-Shirley model [9], one of the BRDFs (Bidirectional Reflectance Distribution Functions), is adopted as a reflecting model of space objects. BRDF is a function describing the ratio of the incident light energy to the reflecting one. Figure 1 shows the reflecting model and unit vectors of the facet.

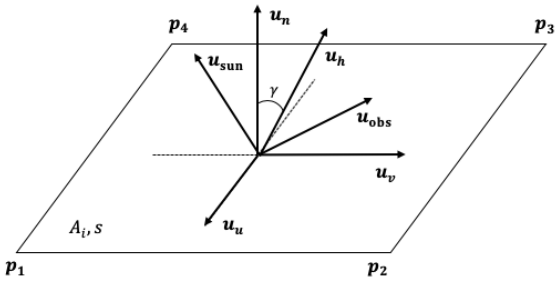

Fig. 1. The reflecting model and unit vectors of the facet.

The rotation of space objects is described with ZYX Euler angles as

$$R_{bi} = [C_\varphi{}^1][C_\theta{}^2][C_\psi{}^3] \tag{3}$$

where

$$[C_\varphi{}^1] = \begin{bmatrix} 1 & 0 & 0 \\ 0 & \cos\varphi & -\sin\varphi \\ 0 & \sin\varphi & \cos\varphi \end{bmatrix}, \quad [C_\theta{}^2] = \begin{bmatrix} \cos\theta & 0 & \sin\theta \\ 0 & 1 & 0 \\ -\sin\theta & 0 & \cos\theta \end{bmatrix}, \quad [C_\psi{}^3] = \begin{bmatrix} \cos\psi & -\sin\psi & 0 \\ \sin\psi & \cos\psi & 0 \\ 0 & 0 & 1 \end{bmatrix}$$

where φ, θ, and ψ are the roll angle, the pitch angle, and the yaw angle respectively. The four points of the square facet after rotation in the body-fixed frame, $\boldsymbol{p}_{(i)} = \left[\boldsymbol{p}_{(i)_1}, \boldsymbol{p}_{(i)_2}, \boldsymbol{p}_{(i)_3}, \boldsymbol{p}_{(i)_4}\right]^T$ is determined by those in the reference frame, $\boldsymbol{p}_{r(i)} = \left[\boldsymbol{p}_{r(i)_1}, \boldsymbol{p}_{r(i)_2}, \boldsymbol{p}_{r(i)_3}, \boldsymbol{p}_{r(i)_4}\right]^T$ and the rotational matrix R_{bi}.

$$\boldsymbol{p}_{(i)} = R_{bi_p}\boldsymbol{p}_{r(i)} \tag{4}$$

$\boldsymbol{u}_{\boldsymbol{u}}$ and $\boldsymbol{u}_{\boldsymbol{v}}$, which defines *i* th facet after the rotation are obtained as

$$\boldsymbol{u}_{u(i)} = \boldsymbol{p}_{(i)_4} - \boldsymbol{p}_{(i)_3} \tag{5}$$

$$\boldsymbol{u}_{v(i)} = \boldsymbol{p}_{(i)_2} - \boldsymbol{p}_{(i)_3} \tag{6}$$

$\boldsymbol{u}_{\boldsymbol{n}}$, the normal vector of the facet is formulated as follows under the assumption of a small facet.

$$\boldsymbol{u}_{n(i)} = \frac{\boldsymbol{u}_{u(i)} \times \boldsymbol{u}_{v(i)}}{\left\|\boldsymbol{u}_{u(i)} \times \boldsymbol{u}_{v(i)}\right\|} \tag{7}$$

The apparent brightness magnitude, which is measured by the observer, is

$$m_{\text{app}} = -26.7 - 2.5\log_{10}\left|\sum_{i=1}^{N}\frac{F_{\text{obs},i}}{C_{\text{sun,vis}}}\right| \tag{8}$$

where -26.7 is the relative magnitude of the Sun, $C_{\text{sun,vis}}$ = 455 W/m^2 is the power per square meter of sunlight striking the target surface, in reference to [6]. *N* is the total facet number. $F_{\text{obs},i}$ is the fraction of the sunlight reflecting *i* th facet and described as

$$F_{\text{obs},i} = \frac{C_{\text{sun,vis}}\rho_{\text{total}(i)}A_{(i)}(\boldsymbol{u}_{\mathbf{sun}} \cdot \boldsymbol{u}_{n(i)})(\boldsymbol{u}_{\mathbf{obs}} \cdot \boldsymbol{u}_{n(i)})}{{h_{\text{d}}}^2} \tag{9}$$

where $\rho_{\text{total}(i)}$ is the BRDF of *i* th face. h_{d} is distance from the observer to the target, and A_i is area of *i* th facet. Given the position of the Sun and the observer is fixed, $F_{\text{obs},i}$ depends on attitude, shape, and specular reflectance of space objects. It indicates that this term is very important in state estimation using light curves. It should be noted that the facet cannot reflect a sunlight when the angle between $\boldsymbol{u}_{\mathbf{sun}}$ and $\boldsymbol{u}_{n(i)}$, $\boldsymbol{u}_{\mathbf{obs}}$ and $\boldsymbol{u}_{n(i)}$ becomes above 90 degree.

$$\boldsymbol{u}_{\mathbf{sun}} \cdot \boldsymbol{u}_{n(i)} > 0 \quad \text{and} \quad \boldsymbol{u}_{\mathbf{obs}} \cdot \boldsymbol{u}_{n(i)} > 0 \tag{10}$$

Apparent area, which is projected to the observer direction, is

$$A_{vis} = \sum_{i=1}^{N} A_{(i)}(\boldsymbol{u}_{n(i)} \cdot \boldsymbol{u}_{\mathbf{obs}}) \tag{11}$$

2.2 Quasi-static Light Curve Model

Quasi-static Light Curve Model calculates magnitude and γ taking account of moment of inertia of space objects. Light curves can be obtained by substituting Euler angles, calculated by moment of inertia as an input, into Static Light Curve Model. In other words, Quasi-static Light Curve Model relates light curves to dynamics of space objects.

Dynamics of space objects are calculated by the following Eq. 12-16. Firstly, angular velocity is obtained by Euler equations shown in Eq. 12, regarding space objects as rigid body.

$$\begin{Bmatrix} I_x\dot{w}_x \\ I_y\dot{w}_y \\ I_z\dot{w}_z \end{Bmatrix} = \begin{Bmatrix} (I_y - I_z)w_y w_z + T_x \\ (I_z - I_x)w_z w_x + T_y \\ (I_x - I_y)w_x w_y + T_z \end{Bmatrix} \tag{12}$$

where I_x, I_y, and I_z represent moment of inertia, w_x, w_y, and w_z are angular velocity in the body-fixed frame, and T_x, T_y, and T_z are external torque in the body-fixed frame, respectively. This model considers gravity gradient torque, solar radiation torque, and aerodynamic torque. Differential equation of attitude angles ignoring products of inertia is expressed with

$$\begin{Bmatrix} \dot{\varphi} \\ \dot{\theta} \\ \dot{\psi} \end{Bmatrix} = [A]^{-1} \left(\boldsymbol{w} - [Q] \begin{Bmatrix} \omega_r \\ \omega_s \\ \omega_w \end{Bmatrix} \right) \tag{13}$$

Attitude angles are formulated by substituting angular velocities obtained in Eq. 12 into Eq. 13, and numerical integration with Runge-Kutta. Matrix A and Q are defined as

$$[A] = \begin{bmatrix} 1 & 0 & -\sin\theta \\ 0 & \cos\varphi & \sin\varphi\cos\theta \\ 0 & -\sin\varphi & \cos\varphi\cos\theta \end{bmatrix} \tag{14}$$

$$[Q] = \left[C_\varphi{}^1\right]\left[C_\theta{}^2\right]\left[C_\psi{}^3\right] \begin{bmatrix} 0 & 1 & 0 \\ 0 & 0 & -1 \\ -1 & 0 & 0 \end{bmatrix} \tag{15}$$

In addition, ω_r, ω_s, and ω_w represent acceleration of RSW coordinate. This paper assumes a circular orbit with altitude of 600 km without perturbations, that is, $\omega_w = n$ and $F_w = 0$.

$$\begin{Bmatrix} \omega_r \\ \omega_s \\ \omega_w \end{Bmatrix} = \begin{Bmatrix} rF_w/h \\ 0 \\ h/r^2 \end{Bmatrix} = \begin{Bmatrix} 0 \\ 0 \\ n \end{Bmatrix} \tag{16}$$

where r is the norm of position vector from geocentric to the target, h is angular momentum of the orbit, and n is mean motion.

3 Result and Discussion

This section shows the results by two light curve models. Cubesat model shown in Figure 2 is used as a target. x_b, y_b, and z_b represent the body-fixed frame, and L is the length of a side. The definition of the facets is summarized in Table 1.

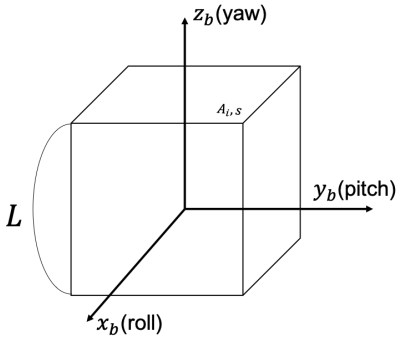

Fig. 2. Cubesat model.

Table 1. The definition of the facets.

Direction	$-z_b$	$+x_b$	$+y_b$	$-x_b$	$-y_b$	$+z_b$
Facet number	Facet 1	Facet 2	Facet 3	Facet 4	Facet 5	Facet 6

3.1 Static Light Curve Model

This section represents the results by Static Light Curve Model. Four cases are simulated by changing parameters, such as the angle between the sun directional vector ($\boldsymbol{u}_{\mathbf{sun}}$) and the observer vector ($\boldsymbol{u}_{\mathbf{obs}}$), the length of a side, and specular reflectance. The cubesat model is rotated in 360 degree about roll axis (x_b) in each case. Simulation conditions are shown in Table 2.

Table 2. Simulation conditions of Static Light Curve Model.

	Case 1	Case 2	Case 3	Case 4
The length of a side, L	1 m	1 m	2 m	1 m
The angle between $\boldsymbol{u}_{\mathbf{sun}}$ and $\boldsymbol{u}_{\mathbf{obs}}$	0 deg	90 deg	0 deg	0 deg
Specular reflectance, s	0.7	0.7	0.7	0.3

Figure 3 represents the light curves and γ of Case 1 and Case 2, respectively. Glint can be detected once every 90 degrees in both cases. It is the moment that γ becomes zero, in other words, $\boldsymbol{u}_{\boldsymbol{h}}$ coincides with $\boldsymbol{u}_{\boldsymbol{n}}$. Figure 4 is the light curve and apparent area of Case 3. The peak of glint in Case 3 becomes higher than that of Case 1. Figure 5 is the light curve of Case 4. The peak of glint in Case 4 becomes lower and the shape is a little different from Case 1. However, the moments of glint detection of both Case 3 and Case 4 are the same as that of Case 1.

From these results, parameters for the glint detection is only γ. Apparent areas and specular reflectance cannot be constrains of glint detection but affect the peak and the shape of glint. Figure 6 shows the range of γ of glint detection. It can be approximately determined as 0<γ<7 degrees in Ashikhmin-Shirley model. This geometric constrained condition enables to obtain the range of Euler angles where they should exist. It makes it possible to improve state estimation accuracy using geometry constrains of glint. In regarding attitude angles at the time of glint as initial values, it is possible to exclude meaningless values from initial value candidates by setting initial attitude angles so that γ within the range. In addition, a high-accurate estimation can be performed regardless of the initial values by efficient update of states and covariance matrix with this constrain in the update step of the estimation filter.

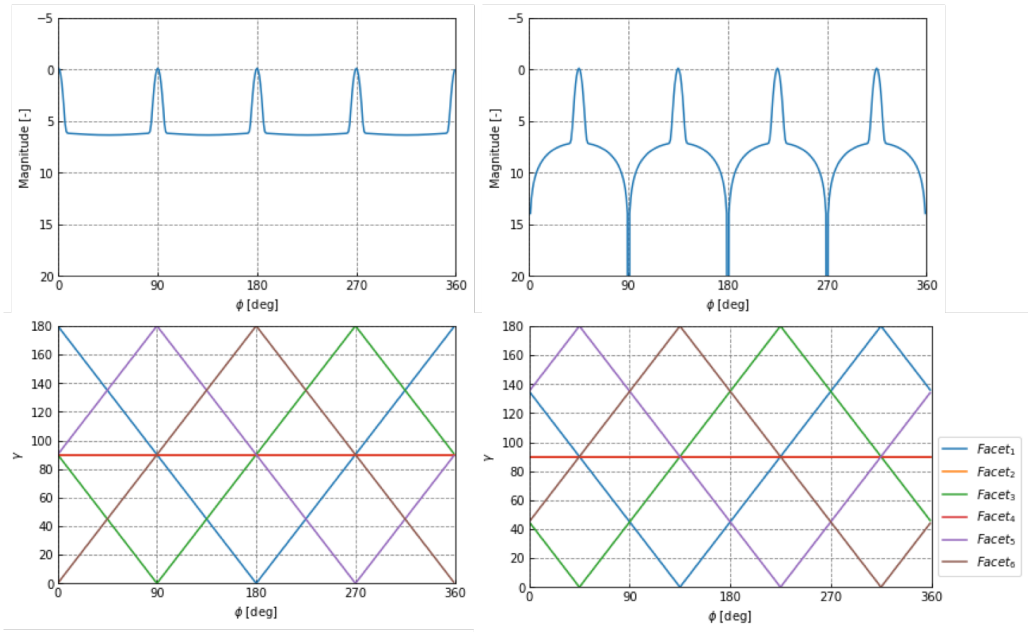

Fig. 3. Light curves and γ of Case 1 and Case 2.

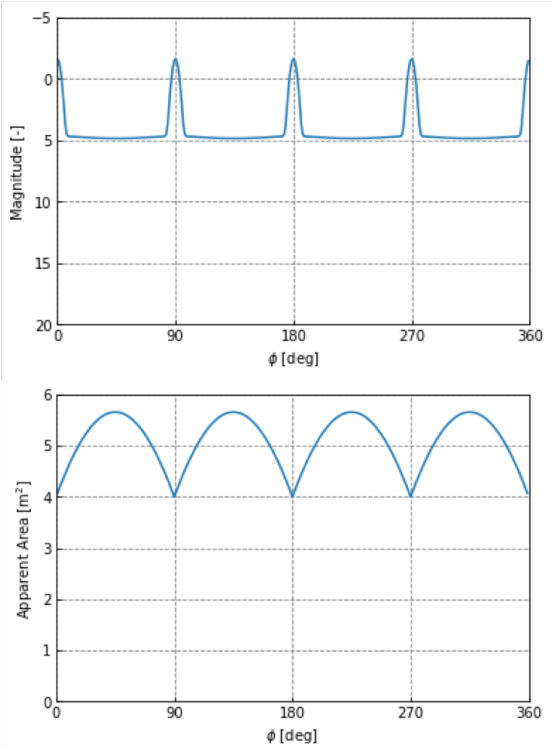

Fig. 4. Light curve and apparent area of Case 3.

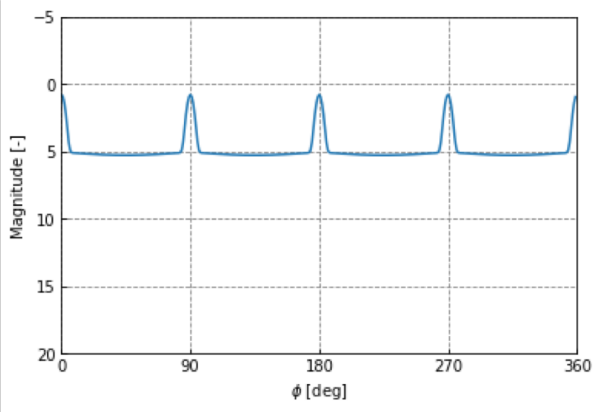

Fig. 5. Light curve of Case 4.

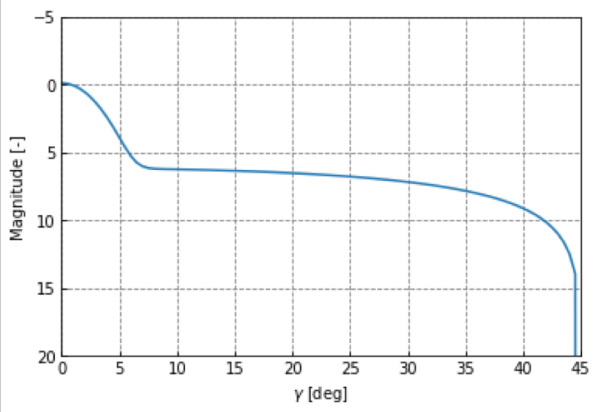

Fig. 6. The range of γ of glint detection.

3.2 Quasi-static Light Curve Model

This section represents the results by Quasi-static Light Curve Model. Two cases are simulated by changing moment of inertia. Simulation conditions are shown in Table 3. Initial attitude angles are $[\varphi, \theta, \psi] = [10, 20, 30]$ deg, initial angular velocities are $[w_x, w_y, w_z] = [0.4, 0.4, 0.4]$ rad/sec, specular reflectance of each facet (s) is 0.7, and the length of a side (L) is 1 m.

Figure 7 represents the light curves and γ of Case 5 and Case 6, respectively. The rotational axis is changing in Case 5, the case of the different moment of inertia in three axes. In contrast, it is a periodic rotation about one axis in Case

6, the case of the same moment of inertia in three axes. Glint is detected in both cases, although the facets of glint are different in two cases. The facets of glint detection in Case 5 are Facet 2 and Facet 4 and that in Case 6 is Facet 6.

It is difficult to determine the facet of glint only by light curves in the case that the model is composed of multiple facets. However, taking into account of dynamics of space objects make it possible to determine the facet of glint detection. It helps attitude estimation of complicated space objects. In addition to this, this qualitative understanding of dynamics is a constraint on the system model of the estimation filter. In other words, the attitude change of the spacecraft is continuous and does not change suddenly even during glint, while the magnitude as the observation model suddenly changes.

Table 3. Simulation conditions of Quasi-static Light Curve Model.

	Case 5	Case 6
Moment of inertia, (I_x, I_y, I_z)	(80, 60, 40) kgm^2	(80, 80, 80) kgm^2

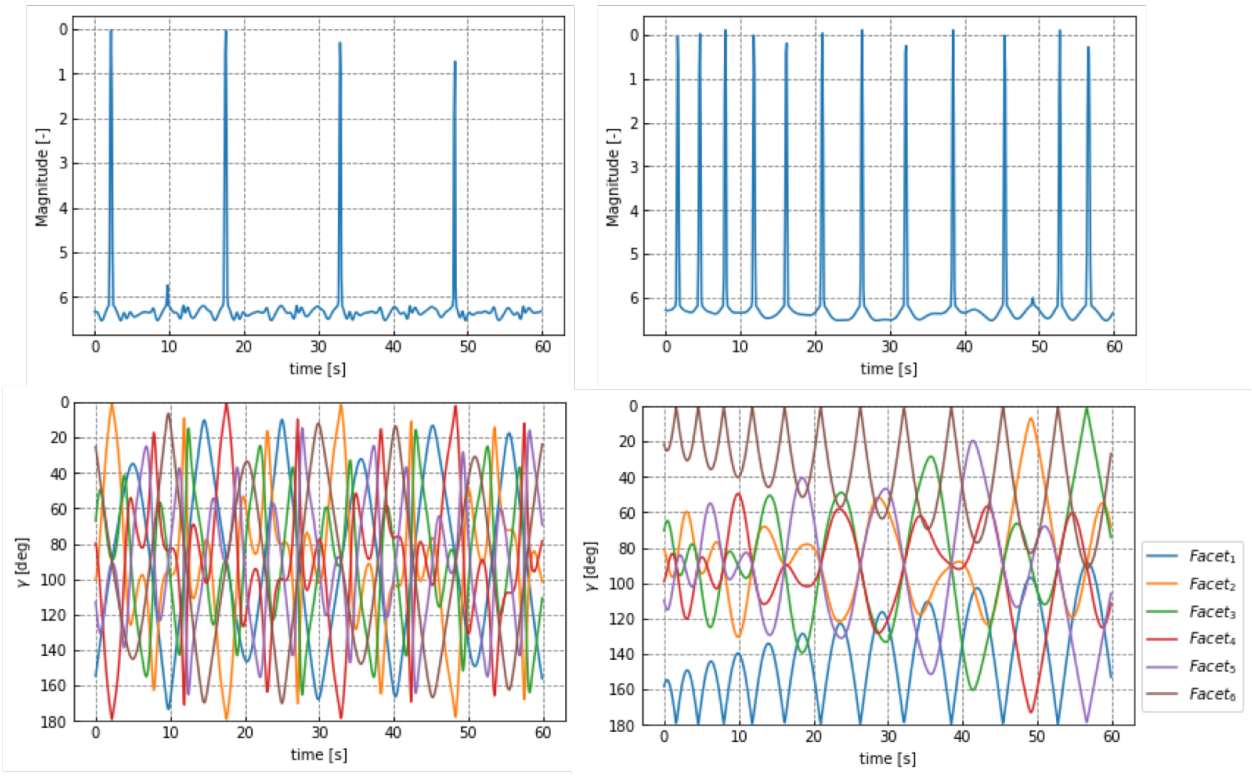

Fig. 7. Light curves and γ of Case 5 and Case 6.

4 Conclusion

This paper determines constrained conditions of glint detection to realize the high-accurate state estimation focusing on glint. Parameters governing the glint detection is only γ, which is the geometry constrained conditions among the Sun, the observer, and the space object. Apparent areas and specular reflectance affect the peak and the shape of glint. In addition, qualitative dynamics of space objects enables to become a constraint in system model of the estimation filter, as well to determine the facet detected glint in complicated objects composed of multiple facets. By

using two constraints in glint detection, high-accurate state estimation technique focusing on glint will be established as future work.

5 References

1. Liou, J.-C., "An active debris removal parametric study for LEO environment remediation," *Advances in Space Research,* vol. 47, no. 11, pp. 1865-1876, 2011.
2. Toshiya Enomoto, Toshiya Hanada, Koki Fujita, and Yukihiko Kitazawa, “Monitoring the health of geosynchronous spacecraft using photometric observations”, Paper IAC-16, A6, IP,23,x34674.
3. Johanna Torppa, “Lightcurve inversion for asteroid spins and shapes”, PhD thesis, University of Helsinki, 2007.
4. Toshiya Enomoto, ”Estimation of Space Object Behaviour Using Optical Measurements,” Master Thesis, Kyushu University, 2016.
5. Kazufumi Watanabe, Koki Fujita, and Toshiya Hanada, “Dynamic Observation of Space Objects Using Adaptive Optics Simulation and Light Curve Analysis”, The 2016 AMOS Technical Conference Proceedings
6. Joanna C. Hinks, Richard Linares, John L. Crassidis, “Attitude Observability from Light Curve Measurement,” AIAA Guidance, Navigation, and Control Conference, Boston, August 19-22, 2013.
7. Joanna C. Hinks and John L. Crassidis, “Angular Velocity Bounds via Light Curve Glint Duration,” AIAA Guidance, Navigation, and Control Conference San Diego, USA, January 1-4, 2016.
8. Michael A. Earl et al., "Estimating the spin axis orientation of the Echostar-2 box-wing geosynchronous satellite," *Advances in Space Research,* vol. 61, no. 8, pp. 2135-2146, 2018.
9. Michael Ashikhmin, and Peter Shirley, "An Anisotropic Phong Light Reflection Model," *Journal of Graffic Tools,* vol. 5, no. 2, pp. 25-32, 2000.